Struct Multidisc Optim
DOI 10.1007/s00158-007-0138-y

RESEARCH PAPER

Topology optimization of beam cross-section considering warping deformation

Shutian Liu · Xiaomin An · Haipeng Jia

Received: 14 August 2006 / Revised: 24 February 2007 / Accepted: 25 March 2007
© Springer-Verlag 2007

Abstract The beam cross-section optimization problems have been very important as beams are widely used as efficient load-carrying structural components. Most of the earlier investigations focus on the dimension and shape optimization or on the topology optimization along the axial direction. An important problem in beam section design is to find the location and direction of stiffeners, for the introduction of a stiffener in a closed beam section may result in a topologically different configuration from the original; the existing section shape optimization theory cannot be used. The purpose of this paper is to formulate a section topology optimization technique based on an anisotropic beam theory considering warping of sections and coupling among deformations. The formulation and corresponding solving method for the topology optimization of beam cross-sections are proposed. In formulating the topology optimization problem, the minimum averaged compliance of the beam is taken as objective, and the material density of every element is used as design variable. The schemes to determine the rigidity matrix of the cross-sections and the sensitivity analysis are presented. Several kinds of topologies of the cross-section under different load conditions are given, and the effect of load condition on the optimum topology is analyzed.

Keywords Topology optimization · Beam · Cross-section · Warping · Coupling deformation

S. Liu (✉) · X. An · H. Jia
State Key Laboratory of Structural Analysis for Industrial Equipment and Department of Engineering Mechanics,
Dalian University of Technology,
Dalian 116024, China
e-mail: stliu@dlut.edu.cn

1 Introduction

Beams are very important load-carrying components in engineering structures. For example, the rotor blades of modern helicopters and large wind generators (Giavotto et al. 1983) are typical beam structures. In the design of modern structures, such as aeronautic and astronautic structures, weight reduction is an important requirement besides catering to certain structural performance. Therefore, it is extremely concerned to design structural formations of beams by investigating the optimization techniques. At present, for the structural design of beams, the focus is mainly on the dimensions, shape optimization (Banichuk and Karihaloo 1976; Dems 1980; Gracia and Doblare 1988; Mota et al. 1984; Banichuk et al. 2002), and the topology optimization in the domain covered by the longitudinal direction and altitude direction (Bensoe and Kikuchi 1988; Frecker et al. 1997; Suzuki and Kikuchi 1991; Sakata et al. 2002; Rosen and Peter 1996). However, topology optimization of beam cross-sections is rarely found in literatures. An article by Kim and Kim (2000) is one of the several papers on topology optimization of the beam's cross-section and may be the earliest work about this problem. In fact, it is very meaningful and important to process the topology optimization of the beam's cross-section. For example, in the design of the rotor blades of helicopters or the wings of aircrafts, one of the important problems is to find the location and direction of stiffeners because the external profile (the shape and dimension) of the cross-section usually cannot be modified because of the aeroelastic design requirement, only stiffening inside the beam's cross-section is allowed to modify. As the introduction of stiffener in a closed section beam may result in a topologically different configuration from the original cross-section, the existing section shape optimization

cannot be used. Therefore, an advanced technique is required to optimize the cross-section configuration. Topology optimization is an effective technique to find a rational configuration of cross-sections, which can provide a scientific instruction for the structural schematic design and make designers have a rational choice for the complex structure or component at the stage of conceptual design (Rosen and Peter 1996).

It is needed to determine the property of the beam's cross-section based on an appropriate beam theory in the optimization design process. Based on the assumptions of classical Euler–Bernoulli theory or Timoshenko theory, the beam cross-sections will keep the plane during deforming; consequently, the bending rigidity can be expressed by the product of inertia moment of the cross-section and Young's modulus. However, these theories are not appropriate to determine the cross-section property in topology optimization owing to the fact that the cross-section's warping and deformation coupling will happen if the shape of the cross-section is not circular, and/or the material is anisotropic and heterogeneous. Because the topological configuration of the cross-section is obtained by designing the distribution of materials in the design domain (Bensoe and Kikuchi 1988; Frecker et al. 1997; Suzuki and Kikuchi 1991; Sakata et al. 2002; Bendsøe 1989; Rietz 2001; Bendsøe and Sigmund 1999), this distribution is not homogeneous, and the equivalent material constants may be anisotropic. Therefore, an anisotropic beam theory with the consideration of the cross-section's warping and deformation coupling is required.

In this paper, the topology optimization is formulated as minimizing the averaged compliance of the beam by designing the distribution of materials in the design domain of the cross-section. The material densities of the discretized elements with porous materials are taken as design variables. Based on the idea of the solid isotropic material with penalization (SIMP; Bendsøe 1989; Rietz 2001; Bendsøe and Sigmund 1999) method, a power law is used for the relation between the material density of each element and the effective material properties. The rigidity matrix of the cross-section and its sensitivity with respect to design variables are obtained using a finite element model of an anisotropic beam theory considering the cross-section warping and deformation coupling developed by Giavotto et al. (1983). As numerical examples, several typical designs of the beam's cross-section under different load conditions are presented, and the effect of different load conditions on the optimum topology is analyzed.

2 Stiffness of cross-section

Consider a beam with generalized cross-section subject to bending and twisting moments and shear and axial forces. The geometry, the coordinate, and the inner forces acted on the cross-section are shown in Fig. 1. Based on the idea of the article by Giavotto et al. (1983), displacement $\{\boldsymbol{s}\}$ of a general point is resolved into a part $\{\boldsymbol{v}\}$, which does not strain the sections, and residual part $\{\boldsymbol{g}\}$, which is called warping displacement, by putting $\{\boldsymbol{s}\}=\{\boldsymbol{v}\}+\{\boldsymbol{g}\}$. The first part can be expressed in terms of the translation displacement $\{\boldsymbol{w}\}$ and rotational displacement $\{\varphi\}$ as:

$$\begin{aligned} &\{v\} = \{w\} + [z]\{\varphi\},\ \{w\} = \{w_1, w_2, w_3\}^T, \\ &\{\varphi\} = \{\varphi_1, \varphi_2, \varphi_3\}^T \end{aligned} \tag{1}$$

$$[z] = \begin{bmatrix} 0 & 0 & -x_2 \\ 0 & 0 & x_1 \\ x_2 & -x_1 & 0 \end{bmatrix} \tag{2}$$

The warping displacement is discretized on the section through $\{\boldsymbol{g}\}=[\mathbf{N}]\{\boldsymbol{\Gamma}\}$. Here, column $\{\boldsymbol{\Gamma}\}$ contains the nodal warping displacement components, and $[\mathbf{N}]$ is the general shape function matrix, which can be defined in each element. The displacement of a general point can be described in terms of $\{\boldsymbol{w}\}$, $\{\varphi\}$, and $\{\boldsymbol{\Gamma}\}$.Defining a strain operator as follows:

$$[\partial L] = \begin{bmatrix} \frac{\partial}{\partial x_1} & 0 & \frac{\partial}{\partial x_2} & 0 & 0 & 0 \\ 0 & \frac{\partial}{\partial x_2} & \frac{\partial}{\partial x_1} & 0 & 0 & 0 \\ 0 & 0 & 0 & \frac{\partial}{\partial x_2} & \frac{\partial}{\partial x_1} & 0 \end{bmatrix}^T, \tag{3}$$

$$[S] = \begin{pmatrix} 0 \\ I \end{pmatrix}$$

then, the strain of any point can be expressed in the following form:

$$\begin{aligned} &\{\varepsilon\} = [B]\{\Gamma\} + [S][N]\{\Gamma'\} + [Z]\{\Psi\}, \\ &\{\sigma\} = [D]\{\varepsilon\} \end{aligned} \tag{4}$$

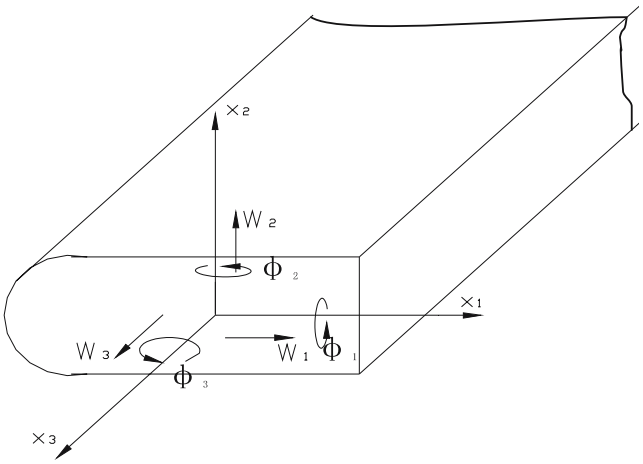

Fig. 1 Coordinate system of the beam

Here, [**D**] is the elastic matrix of the material. Superscript $(\bullet)'$ represents the derivative with respect to x_3. **I** represents three-order unit matrix. Matrices [**B**] and [**Z**] are defined by

$$[\mathbf{B}] = [\partial\mathbf{L}][\mathbf{N}],\ [\mathbf{Z}] = \begin{bmatrix} (0)_{3\times3} & (0)_{3\times3} \\ \mathbf{I}_{3\times3} & z \end{bmatrix} \tag{5}$$

According to the virtual work principle, the governing equations of the beam have the following form:

$$\begin{bmatrix} M & 0 \\ 0 & 0 \end{bmatrix}\begin{Bmatrix} \Gamma'' \\ \Psi'' \end{Bmatrix} - \begin{bmatrix} H & -L \\ L^{\mathrm{T}} & 0 \end{bmatrix}\begin{Bmatrix} \Gamma' \\ \Psi' \end{Bmatrix} - \begin{bmatrix} E & R \\ R^{\mathrm{T}} & A \end{bmatrix}\begin{Bmatrix} \Gamma \\ \Psi \end{Bmatrix} + \begin{Bmatrix} 0 \\ \theta \end{Bmatrix} = 0 \tag{6}$$

Where $\{\theta\}$ and $\{\Psi\}$ are the resultant forces of the section and the general strain parameters, respectively

$$\{\theta\} = (Q_1, Q_2, Q_3, M_1, M_2, M_3)^{\mathrm{T}},$$
$$\{\Psi\} = \begin{Bmatrix} w' + [t]\{\varphi\} \\ \varphi' \end{Bmatrix},\ [t] = \begin{bmatrix} 0 & -1 & 0 \\ 1 & 0 & 0 \\ 0 & 0 & 0 \end{bmatrix} \tag{7}$$

Here $Q_1(Q_2)$ and Q_3 are the resultant shear force and the axial force of the section respectively, and $M_1(M_2)$ and M_3 are the bending and twisting moment of the section. The coefficient matrices in (6) are defined as follows:

$$[\mathbf{M}] = \int_A [\mathbf{N}]^{\mathrm{T}}[\mathbf{S}]^{\mathrm{T}}[\mathbf{D}][\mathbf{S}][\mathbf{N}][\mathbf{Z}]dA,\quad [\mathbf{L}] = \int_A [\mathbf{N}]^{\mathrm{T}}[\mathbf{S}]^{\mathrm{T}}[\mathbf{D}][\mathbf{Z}]dA$$
$$[\mathbf{R}] = \int_A [\mathbf{B}]^{\mathrm{T}}[\mathbf{D}][\mathbf{Z}]dA,\quad [\mathbf{A}] = \int_A [\mathbf{Z}]^{\mathrm{T}}[\mathbf{D}][\mathbf{Z}]dA$$
$$[\mathbf{E}] = \int_A [\mathbf{B}]^{\mathrm{T}}[\mathbf{D}][\mathbf{B}]dA,\quad [\mathbf{C}] = \int_A [\mathbf{B}]^{\mathrm{T}}[\mathbf{D}][\mathbf{S}][\mathbf{N}]dA,\quad [\mathbf{H}] = [\mathbf{C}] - [\mathbf{C}]^{\mathrm{T}} \tag{8}$$

The solutions of (6) can be divided into two parts: one is the end solutions, which only affect a small domain at the end of the beam, and the other is the central solutions, which affect the most part of the domain away from the ends of the beam. Therefore, the central solutions are taken as the deformation pattern of the beam cross-sections. The central solutions are determined by the following equations (Giavotto et al. 1983):

$$\begin{bmatrix} \mathbf{E} & \mathbf{R} \\ \mathbf{R}^{\mathrm{T}} & \mathbf{A} \end{bmatrix}\begin{Bmatrix} \Gamma \\ \Psi \end{Bmatrix} = \begin{bmatrix} -\mathbf{H} & \mathbf{L} \\ -\mathbf{L}^{T} & \mathbf{0} \end{bmatrix}\begin{Bmatrix} \Gamma' \\ \Psi' \end{Bmatrix} + \begin{Bmatrix} 0 \\ \theta \end{Bmatrix} \tag{9}$$

$$\begin{bmatrix} \mathbf{E} & \mathbf{R} \\ \mathbf{R}^{\mathrm{T}} & \mathbf{A} \end{bmatrix}\begin{Bmatrix} \Gamma' \\ \Psi' \end{Bmatrix} = \begin{Bmatrix} 0 \\ \theta' \end{Bmatrix} \tag{10}$$

$$\text{here, } \{\theta'\} = \begin{bmatrix} 0 & 0 \\ -t & 0 \end{bmatrix}\{\theta\} \tag{11}$$

(9) and (10) are linear, their central solutions have the following forms:

$$\{\Gamma\} = [\mathbf{X}]\{\theta\},\ \{\Gamma'\} = [\mathbf{X}']\{\theta\},$$
$$\{\Psi\} = [\mathbf{Y}]\{\theta\},\ \{\Psi'\} = [\mathbf{Y}']\{\theta\} \tag{12}$$

Substituting expressions (12) into (9) and (10) yields

$$\begin{bmatrix} \mathbf{E} & \mathbf{R} \\ \mathbf{R}^{\mathrm{T}} & \mathbf{A} \end{bmatrix}\begin{Bmatrix} \Gamma' \\ \Psi' \end{Bmatrix} = \begin{Bmatrix} 0 \\ \theta' \end{Bmatrix} \tag{13}$$

$$\begin{bmatrix} \mathbf{E} & \mathbf{R} \\ \mathbf{R}^{\mathrm{T}} & \mathbf{A} \end{bmatrix}\begin{Bmatrix} \mathbf{X}' \\ \mathbf{Y}' \end{Bmatrix} = \begin{bmatrix} \mathbf{0} & \mathbf{0} \\ -t & \mathbf{0} \end{bmatrix} \tag{14}$$

The compliance matrix [**F**] of the section can be defined by:

$$\{\delta\theta\}^{\mathrm{T}}[\mathbf{F}]\{\theta\} = \int_A \{\sigma\}^{\mathrm{T}}\{\delta\varepsilon\}dA \tag{15}$$

Considering (4), (12), and (15), we have:

$$[\mathbf{F}] = \left[X^{\mathrm{T}}, X'^{\mathrm{T}}, Y^{\mathrm{T}}\right]\begin{bmatrix} \mathbf{E} & \mathbf{C} & \mathbf{R} \\ \mathbf{C}^{\mathrm{T}} & \mathbf{M} & \mathbf{L} \\ \mathbf{R}^{\mathrm{T}} & \mathbf{L}^{\mathrm{T}} & \mathbf{A} \end{bmatrix}\begin{bmatrix} X \\ X' \\ Y \end{bmatrix} \tag{16}$$

where, unknown quantities **X**, **Y**, and **X**′ are gotten by solving (13) and (14). The corresponding stiffness matrix of the section is obtained by: $[\mathbf{K}]=[\mathbf{F}]^{-1}$.

3 Formulation of topology optimization problem

For the design of the beam, there is always a concern on how to reduce the weight and improve the stiffness of the beam. In this paper, the objective is to minimize the average compliance of the beam, and the optimal cross-section configuration is obtained by designing the distribution of material in the cross-section. According to the general idea of the topology optimization (Bendsøe 1989), the design domain is discretized by finite elements. The material of each element is considered as a kind of porous material that is made of the solid material and holes, and the equivalent property of this kind of material depends on the property of the material and the porous fraction. Thus, the topology optimization can be accomplished by designing the density of each element. Therefore, the density of each element ρ_i (i=1, 2,...N_e, N_e is the element number) is taken as design variable.

According to the idea of the SIMP (Bendsøe 1989; Rietz 2001; Bendsøe and Sigmund 1999) method, it is assumed that the macroscopic property of every element is homogeneous, and Poisson's ratio is independent of the density; Young's modulus E varies with the function of the density as follows:

$$E(\rho) = \rho^{\eta}E_0 \tag{17}$$

here,ρ is the relative density of the porous material, η is the penalty factor, which is greater than zero, and it is assumed to be 3 in this paper.

The averaged compliance of the beam is:

$$\overline{C} = \int_0^L \{\theta\}^{\mathrm{T}}\{\Psi\}dl \tag{18}$$

where, L is the length of the beam, $\{\theta\}_{6\times1}$ and $\{\Psi\}_{6\times1}$ are the resultant forces of the section and the general strain parameters, respectively (see 7).

According to the beam theory, there are following relations between the resultant forces and the strains:

$$[\mathbf{K}]\ \{\Psi\} = \{\theta\}\ or\ [\mathbf{F}]\ \{\theta\} = \{\Psi\} \tag{19}$$

Therefore, the compliance of the beam can also be expressed as the following:

$$\overline{C} = \int_0^L \{\theta\}^{\mathrm{T}}[\mathbf{F}]\{\theta\}dl \tag{20}$$

In this paper, the beam is optimized under the given loads, so the resultant forces $\{\theta\}$ is independent of the design variables, but the compliance matrix [**F**] is the function of the design variables ρ_i.

Because the objective of the topology optimization for the beam's cross-section is to make the beam's stiffness as large as possible under the given material's consumption, the constraints should include the material volume constraint (here is the solid material area constraint):

$$\sum_{i=1}^{N}\rho_i A_i \le A_0 \tag{21}$$

Here, A_0 is the maximum allowable solid material area of the cross-section; A_i is the area of the ith element.

To avoid singularity, holes are filled with rather weaker material, so the material's density of each element is bounded by a lower limit value. When the density reaches this value, the corresponding element's material is deleted. Therefore, the boundary constraints of the design variables are expressed as

$$\rho_{\min} \le \rho_i \le 1.0,\ i = 1,2,\ldots N_e \tag{22}$$

In this paper, the lower limit value is assumed as $\rho_{\min}$= 0.001.

Generally, the topology optimization problem can be described as follows:

$$\begin{aligned}&\text{Find}: \rho_1,\rho_2,\ldots,\rho_{N_e}\\ &\text{Min}: \overline{C} = \textstyle\int_0^L \{\theta\}^T[\mathbf{F}](\rho_1,\rho_2,\ldots,\rho_N)\{\theta\}dl\\ &\text{s.t.}: \textstyle\sum_{i=1}^{N}\rho_i A_i \le A_0\\ &\rho_{\min} \le \rho_i \le 1.0,\quad i = 1,2,\ldots,N\end{aligned} \tag{23}$$

4 Sensitivity analysis

To solve the optimization problem using mathematical programming, it is needed to calculate the sensitivities of the objective function and of the constraint equations. In this paper, the resultant forces $\{\theta\}$ are independent of the design variables, so the sensitivity of the objective function with respect to each design variable is:

$$\begin{aligned}\frac{\partial\overline{C}}{\partial\rho_i} &= \frac{\partial\int_0^L \{\theta\}^{\mathrm{T}}\left[\mathbf{F}\left(\rho_1,\rho_2,\ldots,\rho_{N_e}\right)\right]\{\theta\}dl}{\partial\rho_i}\\ &= \int_0^L \{\theta\}^{\mathrm{T}}\frac{\partial\left[\mathbf{F}\left(\rho_1,\rho_2,\ldots,\rho_{N_e}\right)\right]}{\partial\rho_i}\{\theta\}dl\end{aligned} \tag{24}$$

Therefore, it is needed to calculate the sensitivity of the compliance matrix [**F**] with respect to each design variable.

Differentiating (16) and considering (17), we have:

$$\begin{aligned}\tfrac{\partial\mathbf{F}}{\partial\rho_i} &= \eta\rho_i^{\eta-1}\left[\mathbf{X}^{\mathrm{T}},\mathbf{X}'\mathrm{T},\mathbf{Y}^{\mathrm{T}}\right]\begin{bmatrix}\mathbf{E}_0 & \mathbf{C}_0 & \mathbf{R}_0\\ \mathbf{C}_0^{\mathrm{T}} & \mathbf{M}_0 & \mathbf{L}_0\\ \mathbf{R}_0^{\mathrm{T}} & \mathbf{L}_0^{\mathrm{T}} & \mathbf{A}_0\end{bmatrix}\begin{bmatrix}\mathbf{X}\\ \mathbf{X}'\\ \mathbf{Y}\end{bmatrix}\\ &+\left[\tfrac{\partial\mathbf{X}^{\mathrm{T}}}{\partial\rho_i},\tfrac{\partial\mathbf{X}'\mathrm{T}}{\partial\rho_i},\tfrac{\partial\mathbf{Y}^{\mathrm{T}}}{\partial\rho_i}\right]\begin{bmatrix}\mathbf{E} & \mathbf{C} & \mathbf{R}\\ \mathbf{C}^{\mathrm{T}} & \mathbf{M} & \mathbf{L}\\ \mathbf{R}^{\mathrm{T}} & \mathbf{L}^{\mathrm{T}} & \mathbf{A}\end{bmatrix}\begin{bmatrix}\mathbf{X}\\ \mathbf{X}'\\ \mathbf{Y}\end{bmatrix}\\ &+\left[\mathbf{X}^{\mathrm{T}},\mathbf{X}'^{\mathrm{T}},\mathbf{Y}^{\mathrm{T}}\right]\begin{bmatrix}\mathbf{E} & \mathbf{C} & \mathbf{R}\\ \mathbf{C}^{\mathrm{T}} & \mathbf{M} & \mathbf{L}\\ \mathbf{R}^{\mathrm{T}} & \mathbf{L}^{\mathrm{T}} & \mathbf{A}\end{bmatrix}\begin{bmatrix}\frac{\partial\mathbf{X}}{\partial\rho_i}\\ \frac{\partial\mathbf{X}'}{\partial\rho_i}\\ \frac{\partial\mathbf{Y}}{\partial\rho_i}\end{bmatrix}\end{aligned} \tag{25}$$

To determine the sensitivity of general displacement $\frac{\partial\mathbf{X}}{\partial\rho_i}$, $\frac{\partial\mathbf{Y}}{\partial\rho_i}$, $\frac{\partial\mathbf{X}'}{\partial\rho_i}$, we must differentiate (13) and (14):

$$\begin{aligned}\begin{bmatrix}\mathbf{E} & \mathbf{R}\\ \mathbf{R}^{\mathrm{T}} & \mathbf{A}\end{bmatrix}\begin{Bmatrix}\frac{\partial\mathbf{X}}{\partial\rho_i}\\ \frac{\partial\mathbf{Y}}{\partial\rho_i}\end{Bmatrix} &= -\eta\rho_i^{\eta-1}\begin{bmatrix}\mathbf{E_0} & \mathbf{R_0}\\ \mathbf{R_0^{\mathrm{T}}} & \mathbf{A_0}\end{bmatrix}\begin{Bmatrix}\mathbf{X}\\ \mathbf{Y}\end{Bmatrix}\\ &+\begin{bmatrix}-\mathbf{H} & \mathbf{L}\\ -\mathbf{L}^{\mathrm{T}} & \mathbf{0}\end{bmatrix}\begin{Bmatrix}\frac{\partial\mathbf{X}'}{\partial\rho_i}\\ \frac{\partial\mathbf{Y}'}{\partial\rho_i}\end{Bmatrix}\\ &+\eta\rho_i^{\eta-1}\begin{bmatrix}-\mathbf{H}_0 & \mathbf{L}_0\\ -\mathbf{L}_0^{\mathrm{T}} & \mathbf{0}\end{bmatrix}\begin{Bmatrix}X'\\ Y'\end{Bmatrix}\end{aligned} \tag{26}$$

$$\begin{bmatrix}\mathbf{E} & \mathbf{R}\\ \mathbf{R}^{\mathrm{T}} & \mathbf{A}\end{bmatrix}\begin{Bmatrix}\frac{\partial\mathbf{X}'}{\partial\rho_i}\\ \frac{\partial\mathbf{Y}'}{\partial\rho_i}\end{Bmatrix} = -\eta\rho_i^{\eta-1}\begin{bmatrix}\mathbf{E_0} & \mathbf{R_0}\\ \mathbf{R_0^{\mathrm{T}}} & \mathbf{A_0}\end{bmatrix}\begin{Bmatrix}\mathbf{X}'\\ \mathbf{Y}'\end{Bmatrix} \tag{27}$$

In (25), (26), and (27), coefficient matrices with subscript "0" are those calculated when the ith element related to ρ_i is filled with solid material completely, and others are void. The coefficient matrices of unknown quantities $\frac{\partial\mathbf{X}}{\partial\rho_i}$, $\frac{\partial\mathbf{Y}}{\partial\rho_i}$, $\frac{\partial\mathbf{X}'}{\partial\rho_i}$, $\frac{\partial\mathbf{Y}'}{\partial\rho_i}$ in (26) and (27) are same to ones of **X**, **Y**, **X′**, **Y′** in (13) and (14), so replacing the right

constant terms in (13) and (14) with those in (26) and (27), we can get these unknown quantities easily.

The sensitivity of the constraint (21) is as follows:

$$\frac{\partial\left(\sum_{i=1}^{N}\rho_i A_i - A_0\right)}{\partial\rho_i} = A_i \tag{28}$$

5 Numerical examples

5.1 Cross-section design of a cantilever beam

To verify the validity of the topology optimization in the beam's cross-section design, let us design the topology of the cross-section of a cantilever beam with a 240×240-mm^2 square cross-section. The length of the cantilever beam is L=3,000.0 mm, the shear (vertical) force and twisting moment are loaded at the end of the cantilever beam (shown in Fig. 2). The material is isotropic, and Young's modulus E=200 Gpa, Poisson's ratio μ=0.3.

The objective is to maximize the stiffness of the beam subject to 50% mass constraint. The design domain is discretized by quadrilateral elements; the values of the initial design variables are all 0.5. In this paper, two cases are discussed. Case 1: only vertical force F=10 kN is loaded at the end of the cantilever beam. Case 2: both vertical force F=10 kN and twisting moment T=10 kN/cm are loaded at the end of the cantilever beam.

To illuminate the difference between the beam theory used in this paper and the classical beam theory, a simple example is discussed in the following.

According to the classical beam theory, under the condition of case 1, to maximize the stiffness of the beam (or to minimize the compliance of the beam) is to maximize the following bending rigidity by distributing materials in the cross-section:

$$EI_x = \int_A E\rho^{\eta} y^2 \mathrm{d}A \tag{29}$$

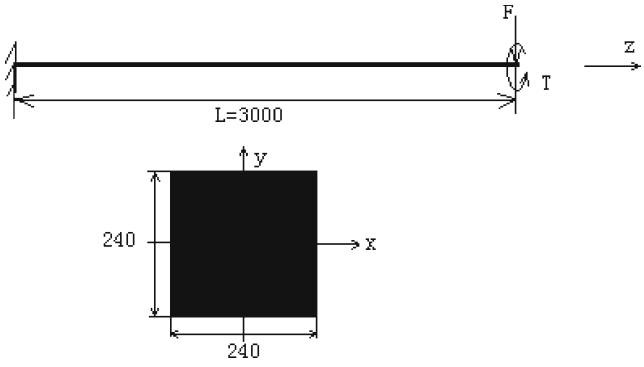

Fig. 2 Model of the cantilever beam

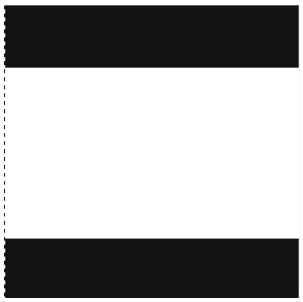

Fig. 3 Topology in case 1 using classical beam theory

Fig. 4 Topology 1: optimal topology in case 1

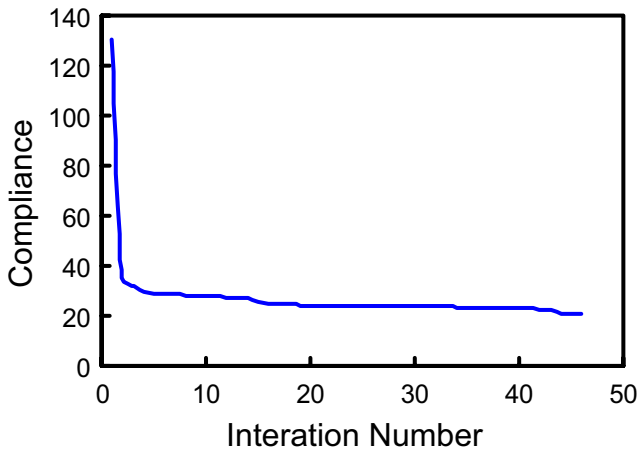

Fig. 5 Topology 2: optimal topology in case 2

Fig. 6 Iterative history of the objective function in case 1

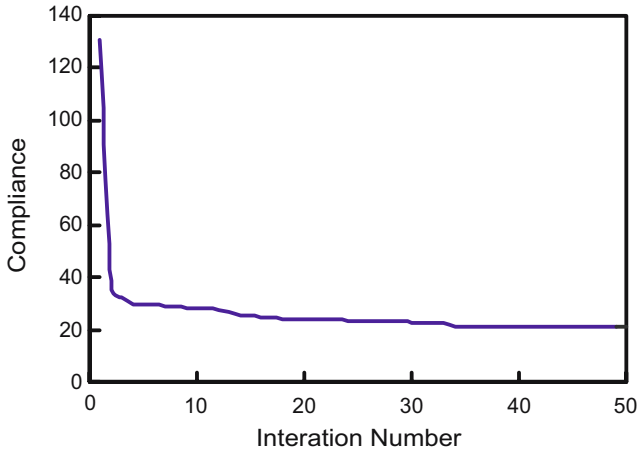

Fig. 7 Iterative history of the objective function in case 2

Fig. 8 Cross-section of I-shape cross-section beam

The optimal cross-section topology is shown in Fig. 3, which has materials at the upper and lower edges, but no materials at the intermediate section. It is obvious that this configuration cannot make the upper and lower flange plates to be an entirety and break the force-transmitting path. The reason for this irrational configuration is that the classical beam theory ignores the shear deformation and the cross-section warping, which will weaken the cross-section rigidity.

Based on the beam theory considering warping of the cross-section and deformation coupling, this drawback can be overcome. Two kinds of optimal cross-section configurations (as shown in Figs. 4 and 5) are obtained using the modified feasible direction method to solve the optimization problem (23). Iterative histories of the objective function under two cases are shown in Figs. 6 and 7, which indicates that the objective function value decreases rapidly at the beginning, then intends to stabilize with the iterations, and finally approaches a constant value.

The optimal results show that the II-shape cross-section makes the averaged compliance minimum under the condition of case 1. However, the I-shape cross-section beam (see Fig. 8) is widely used in engineering. To investigate the property differences between II-shape cross-section beam and I-shape cross-section beam, a comparison is shown in Table 1 under the conditions that

Table 1 Property comparison between II-shape and I-shape cross-sections

	GA_x (10^4kN)	GA_y (10^4kN)	EA (10^4kN)	EI_x (kNmm^2)	EI_y (kNmm^2)	GI_p (kNmm^2)
II-section	113.9	81.6	560	43,633.9	27,553.9	13,056.4
I-section	151.7	75.7	560	43,633.7	19,009.8	1,784.6

Fig. 9 Warping deformation of II-shape and I-shape cross-sections

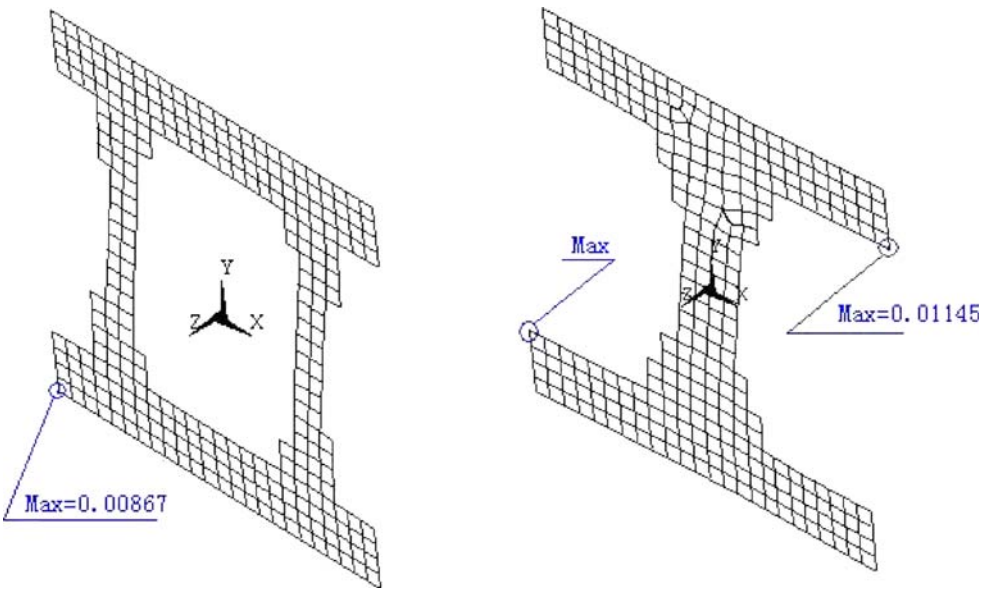

material, cross-section area, beam length, loads, and boundary condition are all the same. Table 1 indicates that the two kinds of cross-sections have equivalent shear rigidity, tensile rigidity, and bending rigidity in the x direction; but the II-shape cross-section beam has larger twisting rigidity than I-shape cross-section beam.

Moreover, comparing the out-of-plane warping displacements, we find that the II-shape cross-section beam has much smaller warping deformation than I-shape cross-section beam (Fig. 9). To verify this, the middle plane on these two kinds of beams is investigated. As shown in Fig. 9, the maximum out-of-plane warping displacement values of II-shape cross-section and I-shape cross-section are 0.00867 and 0.01145 mm, respectively. That shows that the decrease in the section rigidity induced by warping of the II-shape cross-section beam is less than that of the I-shape cross-section beam. Thus, the II-shape cross-section obtained from topology optimization is reasonable.

Comparing two kinds of topology configurations (as shown in Figs. 4 and 5) obtained in different load cases, we can conclude that the load conditions affect the topology configurations extremely. Figure 5 (nonsymmetric configuration) indicates the twisting moment's effects on the topology. To further research the effects of the twisting moment, we enlarge the twisting moment value by ten times and 150 times, respectively. The results are shown in Figs. 10 and 11. From these different configurations, we can generalize the following rules: first, the web plate thickness is reduced (Topology 2 or Topology 4), even degenerating (Topology 3) in the region where two kinds of shear stresses (generated by shear force and twisting moment, respectively) have opposite directions, and the web plate thickness is added (Topology 2 or Topology 4) in the region where two kinds of shear stresses have same directions; second, when the twisting moment value is large enough, the topology configuration becomes a closed-box cross-section (Topology 4) and is nonsymmetric.

Fig. 10 Topology 3: twisting moment is enlarged by ten times in case 2

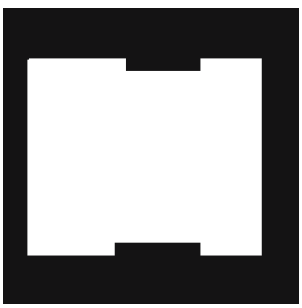

Fig. 11 Topology 4: twisting moment is enlarged by 150 times in case 2

5.2 Thin-walled section reinforcement design

To verify the effectiveness in designing the reinforcement of the thin-walled section, a specific cross-section of a beam considered by Kim and Kim (2000) is designed using the topology optimization technique presented above. The cross-section is shown in Fig. 12, where the beam profile marked by thick solid lines is assumed not to be altered because of its assembly requirement with adjacent structural components. The beam with the length of 150.0 mm is fixed at the left end and loaded by a 1-kN vertical force, a

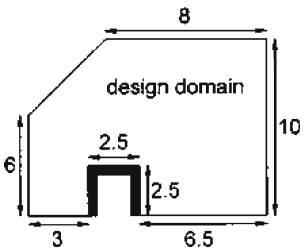

Fig. 12 Initial design domain with a geometric constraint Kim and Kim (2000)

Fig. 13 Section topology obtained by present technique

Fig. 14 Section topology obtained by Kim and Kim (2000)

Table 2 Comparison of cross-sectional rigidities

	Kim and Kim (2000)	This paper
Torsional rigidity(kN mm^2)	3,318.8	4,210.5
Minimum bending moment (kN mm^2)	6,139.8	6,501.2
Maximum bending moment (kN mm^{2}7)	9,831.7	9,173.5

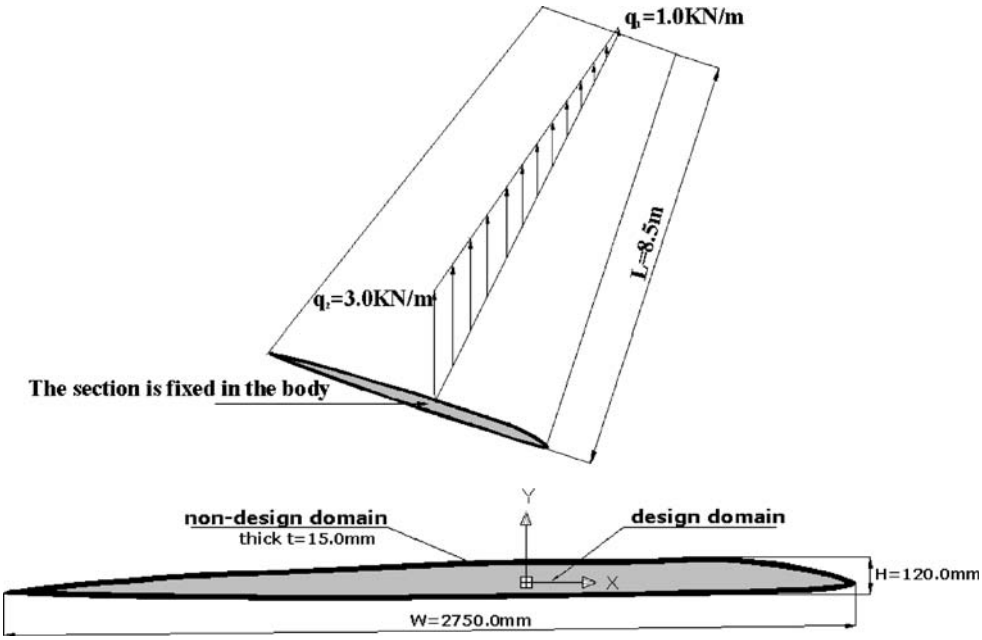

Fig. 15 Geometry, load, and boundary conditions of an aircraft wing

1-kN horizontal force, and a 10^4-kN/mm twisting moment at the right end. The goal of this problem is to find the optimal location and direction of a stiffener in the design domain that lies inside the cross-section profile. The mass constraint requires that the area occupied by the material is less than 40% of the design domain. The objective function is the compliance of the beam. The optimal location and the direction of a stiffener can be identified from the optimal configuration shown in Fig. 13, which is almost the same as that obtained by Kim and Kim (2000) shown in Fig. 14. In addition, the rigidities of both cross-sections are compared in Table 2. This indeed demonstrates the usefulness of the present topology optimization technique in the thin-walled beam section stiffener design.

5.3 Cross-section design of an aircraft wing structure

The wing of an aircraft can be considered as a cantilever beam. The length and the external profile (the shape and dimension) of the cross-section usually cannot be modified because of the aeroelastic design requirements, only stiffening inside the beam's cross-section is allowed to modify. The purpose of this example is to illustrate the effectiveness of topology optimization technique in finding the locations, directions, and dimensions of stiffeners. For simplicity, the constraint includes only the material mass limit, without considering the constraints on the global and/or local buckling of components and on other properties; although these constraints are important for designing the cross-section of wings.

The geometry, load, and boundary conditions of a wing are shown in Fig. 15. The load is the aerodynamic force that is simplified as a linearly varying distributed load along a line with the intensity of 3.0 KN/m at the root and 1.0 KN/m at the free end. The material used has 74 Gpa of Young's modulus and 0.3 of Poisson's ratio. The objective is to obtain a design with minimum compliance by designing the inner structure topology of a typical cross-section with the material constraint ratio of 50% of the design domain. The design domain is an inner area of thin skin with a thickness of 15.0 mm. The change of this skin area is not allowed in the design process to keep the external profile unchanged.

Figure 16 shows the optimal topology of a typical cross-section. Topology optimization gives the stiffener's location and direction. The introduction of the stiffeners changed the topology of the cross-section. It is difficult to obtain this design by conventional shape and/or dimension optimization.

6 Conclusions

Based on an anisotropic beam theory with considering section warping and deformation coupling, topology optimization for the beam's cross-section is achieved. Several kinds of topologies of the cross-section under different load conditions are given, and the effect of load condition on the optimum topology is analyzed. The topology configurations are clear, rational, and practical. In addition, the availability of this technique comparing with the technique using classical beam theory is illustrated through a simple example.

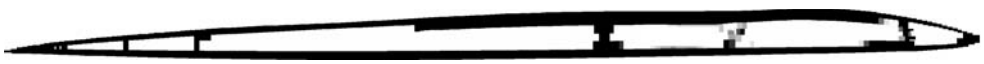

Fig. 16 Optimal topology of a typical cross-section of an aircraft wing

The formulation presented in this paper can be a foundation for the design of beams, considering further complicated conditions met in practical applications, such as the problems with consideration of design-dependent load (such as self weight for slender beams) and multiple load combinations, dynamic effects, and the case of different topologies at different positions along beam axis.

Acknowledgments This research was supported by the National Natural Science Foundation of China through the Grant no. (10332010 and 10421202). It was also supported by the National Basic Research Program of China through Grant no. 2006CB601205 and the Program for New Century Excellent Talents in the University of China (2004). The financial supports are gratefully acknowledged.

References

Banichuk NV, Karihaloo BL (1976) Minimum-weight design of multipurpose cylindrical bars. Int J Solids Struct 12:267–273

Banichuk NV, Ragnedda F, Serra M (2002) Optimum shapes of bar cross-sections. Struct Multidisc Optim 23:222–232

Bendsøe MP (1989) Optimal shape design as a material distribution problem. Struct Optim 1:193–202

Bendsøe MP, Sigmund O (1999) Material interpolation schemes in topology optimization solid mechanics. Ing -Arch 69:635–654

Bensoe MP, Kikuchi N (1988) Generating optimal topologies in structural design using a homogenization method. Comput Methods Appl Mech Eng 71:197–224

Dems K (1980) Multiparameter shape optimization of elastic bars in torsion. Int J Numer Methods Eng 15:1517–1539

Frecker MI, Ananthasuresh GK, Nishiwaki S, Kikuchi N, Kota S (1997) Topological synthesis of compliant mechanisms using multi-criteria optimization. J Mech Des ASME 119:238–245

Giavotto V, Borri M, Mantegazza P, Ghiringhelli G (1983) Anisotropic beam theory and applications. Comput Struct 16:403–413

Gracia L, Doblare M (1988) Shape optimization of elastic orthotropic shafts under torsion by using boundary elements. Comput Struct 30:1281–1291

Kim YY, Kim TS (2000) Topology optimization of beam cross sections. Int J Solids Struct 37:477–493

Mota SC, Rodrigues HC, Oliveira F, LM, Haug EJ (1984) Optimization of the geometry of shafts using boundary elements. J Mech Transm Autom Des 106:199–202

Rietz A (2001) Sufficiency of a finite exponent in SIMP (power law) methods. Struct Multidiscipl Optim 21:159–163

Rosen DW, Peter TJ (1996) The role of topology in engineering design research. Springer, London, pp 81–98

Sakata S, Ashida F, Zako M (2002) Topology and detail geometry optimization for beam structures using homotopy modeling. Comput Methods Appl Mech Eng 191:4279–4293

Suzuki K, Kikuchi N (1991) A homogenization method for shape and topology optimization. Comp Methods Appl Mech Eng 93:291–318